Progress In Electromagnetics Research Letters, Vol. 105, 111–120, 2022

Design of Frequency Multiplexed Coding Metasurface for Dual-Functional Beam Control

Honggang Hao, Qinxuan Ling, Wei Ruan*, and Hanhai Xiao

Abstract—A frequency multiplexed coding metasurface controlling beam is proposed to enrich the functions of a single metasurface. A square F4B dielectric substrate with a copper-clad bottom surface and a V-shaped and quadrangular cross-shaped metal structure is used as the unit. Applying the different responses of x and y polarized waves and optimization of structural parameters, we can obtain 1-bit coding units for the two frequency bands. The reflection phase can be modulated independently of each other. The design of a dual-band metasurface with different beam splitting effects was realized, achieving the goal of different frequency multiplexing functions on a single metasurface. An RCS reduction of 11 dB at 12 GHz and a double beam splitting at 20 GHz with a pitch angle of $\pm 47.6^\circ$ are achieved by metasurface. The test results agree well with the simulation results. The proposed metasurfaces offer a simple structure, low cost, good performance, and promising great applications in areas such as frequency multiplexed communications.

1. INTRODUCTION

Electromagnetic metamaterials can flexibly control EM (electromagnetic) waves by modulating information such as the phase and amplitude in the propagation path [1]. Electromagnetic metasurfaces are two-dimensional spatial forms of electromagnetic metamaterials, also known as new artificial electromagnetic surfaces [2, 3], with advantages such as thinner thickness, smaller size, and lower losses than traditional metasurface. Metasurfaces can realize anomalous reflection [4] and transmission [5], which can be applied to phased array [6], holography [7], and other technology fields.

In 2014, the concept of encoding metasurface was first proposed by Cui's team [8], which combines metasurface with digital information, extending the function of metasurface and increasing the freedom of information. A binary approach is applied in the coding; the unit structures are coded as binary by different phase responses. Then the unit structures are combined in periodic or non-periodic binary sequences on the metasurface to implement various functions [9]. The encoded metasurfaces are divided into 1-bit, 2-bit... n-bit metasurfaces depending on the need for a discrete phase.

In the 1-bit encoded metasurface design, "0" and "1" numbers are represented for two metasurface unit structures with a reflection phase difference of π. Similarly, the n-bit coding method adopts "0,1,... n" numbers to represent the 2^n-units whose unit reflection phase difference is 2π divided by $2n$. The coding metasurface can improve the design speed to a certain extent. Currently, the traditional metasurface is simpler in function through processing, which limits its application. In recent years, multifunctional metasurfaces based on incident wave characteristics have become a hot research field. One of the crucial directions is frequency multiplexed metasurfaces. It has promising applications in areas such as frequency multiplexing communications.

Received 24 April 2022, Accepted 21 June 2022, Scheduled 1 August 2022
* Corresponding author: Wei Ruan (ruanwei@cqupt.edu.cn).
The authors are with the School of Optoelectronic Engineering, Chongqing University of Posts and Telecommunications, Chongqing 400065, China.

In [10], Iqbal et al. proposed a three-layer structured dual-band reflectance hologram metasurface capable of producing two high-quality, low-crosstalk images located at different distances in the X-band and Ku-band near-field channels. In [11], Fu and Liu proposed a dual broadband coding metasurface with polarization conversion, a structure that enables x-polarized and y-polarized wave conversion and RCS reduction in the operating range of dual frequencies. In [12], Li et al. proposed a transmissive dual-band polarization conversion metasurface that converts line polarization incident waves into cross-polarization transmission waves at two frequency points, 7.97 GHz and 17 GHz. At present, simple structure, rich function, and band isolation are influential indexes of the multiplexed metasurface.

In this paper, a design for frequency multiplexed coding reflection metasurface is presented that operates in two commonly used satellite communication bands, 12 GHz and 20 GHz. Firstly, 1-bit coding units for four dual-frequency modes are designed. Then, according to the reflected beam modulation needs, the surface sequence is obtained by the metasurface far-field scattering theory. Finally, employing theoretical analysis and numerical simulation, the beam control function of the metasurface in two frequency bands is discussed and investigated. The measured results demonstrate that the design can achieve the RCS reduction function in the low-frequency band and the beam splitting effect in the high-frequency band.

2. METASURFACE DESIGN

2.1. Design of Unit Structures

According to the 1-bit coding metasurface construction scheme, four units need to be designed to realize multiplexing in two frequency bands. Figs. 1(a) and (b) show schematic diagrams of the unit structure designed in this paper. Each unit element consists of a square F4B ($\varepsilon_r = 2.65$, $\delta = 0.001$) substrate layer with copper metallic V and four-cornered half-cross on it, and a bottom metal copper layer. The parameters of the unit are as follows: thickness $h = 2$ mm, V-shaped tension angle $\theta = 10°$, and period p is taken as 10 mm. The frequency band is a sub-wavelength structure whose operating band and performance are mainly dependent on the superstructure of the metal layer.

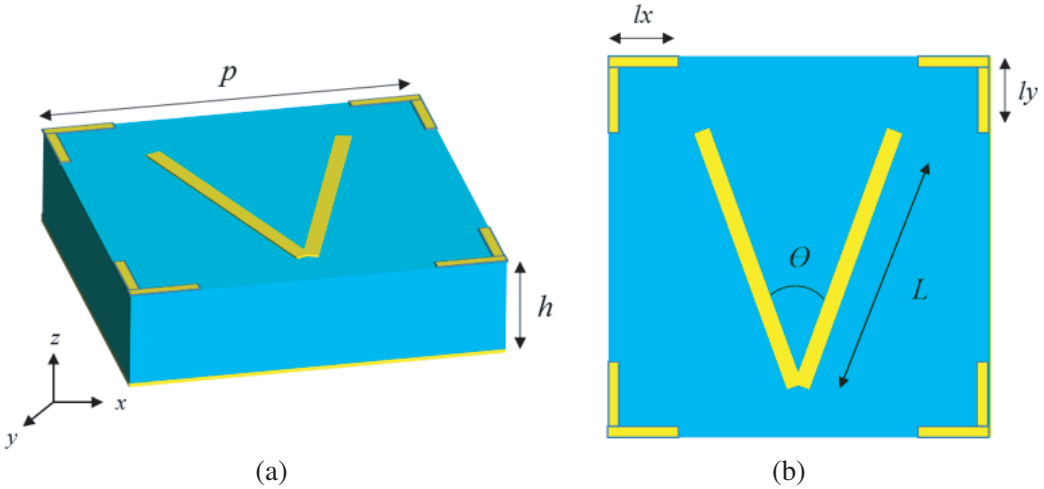

Figure 1. Structure diagram of unit. (a) Construction diagram of unit; (b) Top view of the unit structure.

As shown in Fig. 1(b), the unit structure is symmetrical about the y-axis; thus, the unit response bands to x and y polarized waves are dissimilar. Both the V-shaped and half-cross-shaped structures are similar to dipole structures, which can be compared to a dipole antenna or an oscillator antenna. For dipole antennas, the directional coefficient depends on the arm length L. The gain and directional coefficient are related to the tensor angle θ. For the unit structures in this paper, the reflected phase of the y-polarised incident wave is controlled by the edge length L of the V-shaped structure and the

longitudinal edge length ly of the half-cross-shaped structure. The reflected phase of the x-polarised incident wave is related by the tensor angle θ of the V-shaped structure and the lx of the transverse side of the half-cross structure.

The single-band 1-bit reflective coded metasurface requires the design of 2 units with a phase difference of 180° to the reflected wave, denoted by the numbers 0 and 1, respectively. Theoretical studies and simulations show that the four 1-bit coded metasurface units, 0/0, 0/1, 1/0, and 1/1, operate in the low and high-frequency bands. Before and after "/" are the unit codes of different frequency bands. The amplitude and phase response of the unit can be adjusted independently in the low- and high-frequency bands by adjusting the V-arm length L and half-cross arm length ly, respectively, as shown in Fig. 1. A design for a frequency multiplexed beam-controlled coded metasurface provided by the low-frequency cross-influence between different parameters offers the possibility of realizing a frequency multiplexed beam-controlled coding metasurface. When a y-polarized EM wave is vertically incident, using electromagnetic field simulation software CST, the optimized dimensions of the 1-bit dual-band multiplexed unit structure L and ly can be obtained by adjusting the unit structure parameters, as shown in Table 1. When L and ly are 8 mm and 3.2 mm, respectively, the performance requirements of 0 and 1 coding units operating at low and high frequency can be met simultaneously. Others are similar.

The structural dimensions and coding methods for the four frequency multiplexed metasurface units are given in Tab. 1.

Table 1. Structure parameters of frequency multiplexing unit.

Structural dimensions	Coding method			
	0/0	0/1	1/0	1/1
L/mm	8	8	6.2	6.2
ly/mm	4.4	3.2	4.4	3.2

Simulation results of the coefficients and phase response at y-polarized waves vertical incidence in the low and high-frequency bands are shown in Fig. 2. The reflection coefficients of four units for y-polarized incident waves are above 0.95 in both the 11.6 GHz–13 GHz and 19.8 GHz–21 GHz bands, as illustrated in Figs. 2(a) and (b). Obviously, these elements have high reflective efficiency. When the operating band is 11.6 GHz–13 GHz, 0/* and 1/* approximately satisfy the requirement of 180° phase difference between 1-bit metasurface units 0 and 1. In the meantime, at 19.8 GHz–21 GHz, */0 and */1 also roughly fulfill the requirement of 180° phase difference, as shown in Figs. 2(c) and (d). However, in the subsequent studies of the coding sequence and array, the analysis is focused on the performance at 12 GHz and 20 GHz. The comparative analysis between 0/1 and 0/0, 1/1 and 1/0 units shows that performance is basically consistent between the two bands, and the interaction between the L and ly parameters is small. The unit structure effectively decreases the mutual interference between frequency bands, which ensures the independence and flexibility of frequency multiplex codes.

Notably, after functional setup and surface sequence design aided by the metasurface far-field scattering theory, the elements have good potential to achieve beam-controlled frequency multiplexing functions.

2.2. The Design of Metasurface

The concept of digital coding is applied to coded metasurfaces, in which the stable electromagnetic wave modulation capability of the unit structure is exploited, combined with the metasurface far-field scattering theory. The four frequency multiplexed units are set to different functions at each frequency, and the unit code sequence of each frequency band is obtained to construct the metasurface. Herein, the functions of different frequency reflection beam controlling effects are implemented on the metasurface. The design of this paper is based on the study of square metasurfaces. The metasurface is composed of $N \times N$ subarrays of equal size, each consisting of $r \times r$ "0" or "1" units. When the plane wave is

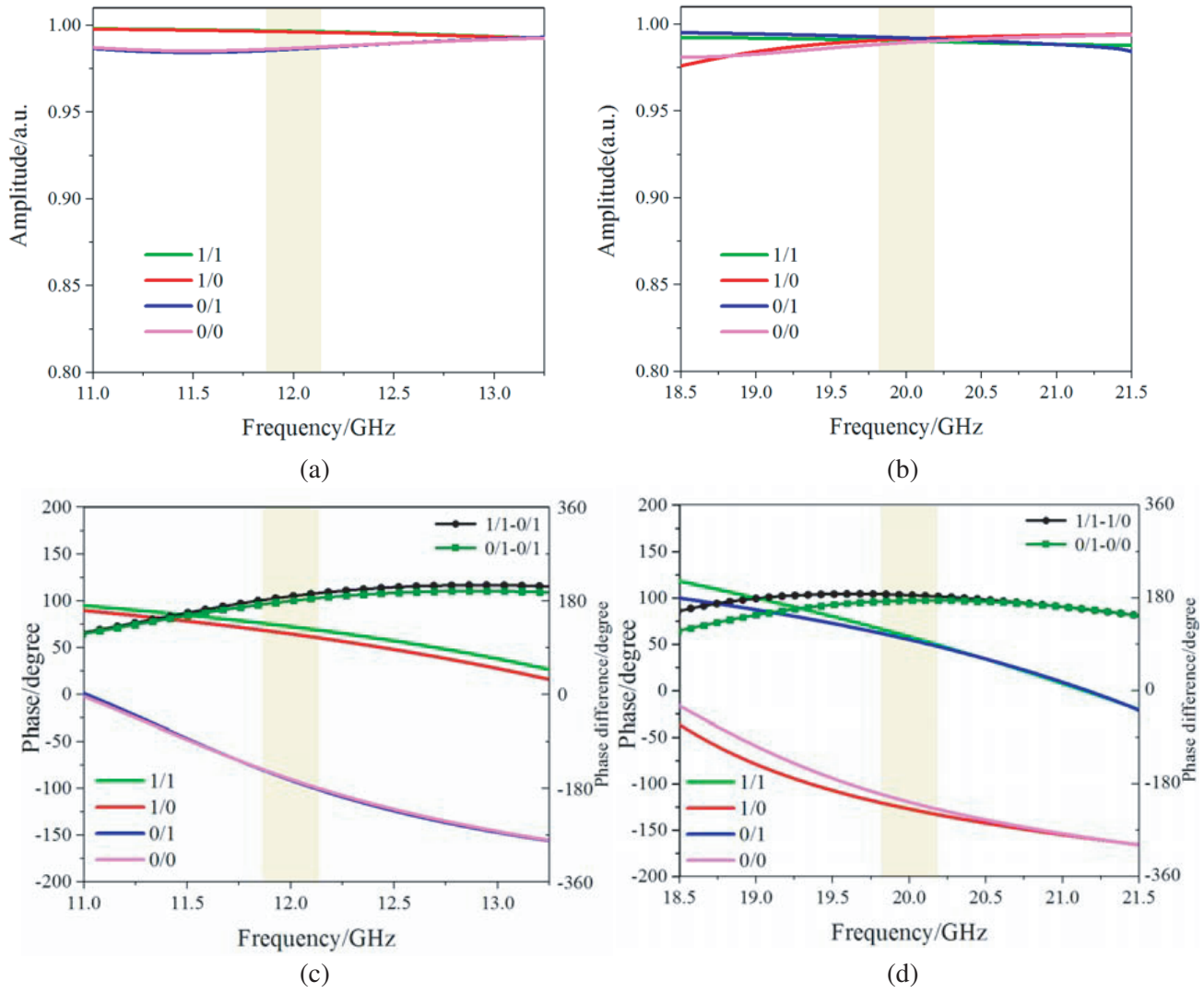

Figure 2. Amplitude and phase responses of the multiplexed unit at different operating frequencies. (a) and (b) Reflection amplitude of the incident wave at low and high-frequency; (c) and (d) Phase response and phase difference of the incident wave at low and high-frequency.

incident vertically, the far-field scattered field at the coding metasurface is [6]:

$$f(\theta,\psi) = f_e(\theta,\psi)\sum_{m=1}^{N}\sum_{n=1}^{N}\exp\{-i\{\psi(m,n) + KD(m-1/2)\sin\theta\cos\psi + KD(n-1/2)\sin\theta\sin\psi\}\} \tag{1}$$

where f_e $(\theta,\ \psi)$ represents the far-field function of the subarray; θ and ψ are the pitch and azimuth angles of the scattered beam; ψ (m,n) is the reflected phase of a single array element; m, n are the array coordinate values; $D = rp$ is the subarray period length of the metasurface; K represents the wave vector. Since the far-field scattering function on the metasurface is determined, such as the number of control beams, angle, and energy ratio, the required unit coding sequence could be theoretically calculated according to Equation (1). The frequency multiplexing units are implemented to perform different beam control functions at different operating frequencies, thus completing the design of the frequency multiplexing coding metasurface.

Theoretical calculations show that the axisymmetric double-reflection beam occurring through the unit structures are spaced along a single direction "010101…". According to the generalized Snell

theorem and the metasurface far-field scattering function, the pitch angle θ and azimuth angle ψ of the reflected beam are related to the unit arrangement [7]:

$$\theta = \sin^{-1}(\lambda/\Gamma) \tag{2}$$

$$\begin{cases} \sin\dfrac{\phi_1+\phi_2}{2} = 1 \\ \cos\dfrac{\phi_1-\phi_2}{2} = 1 \end{cases} \tag{3}$$

$$\phi_1 = 1/2kp(\sin\theta\cos\psi + \sin\theta\sin\psi), \quad \phi_2 = 1/2kp(-\sin\theta\cos\psi + \sin\theta\sin\psi) \tag{4}$$

where λ is expressed as the wavelength of the operating frequency in free space, where Γ is a period of the encoded metasurface in the x-direction. The azimuthal angles $\psi = 0°$, $180°$, and pitch angle $\theta = \sin^{-1}(\lambda/2)$ for the axisymmetric reflected dual-beam are calculated from Equations (3) and (4).

When the unit structures in x and y directions are simultaneously arranged as "010101…", the reflected beam is a centrosymmetric quadruple beam, and the reflected beam pitch angles θ and azimuth angles ψ can be expressed as [7]:

$$\theta = \sin^{-1}\left(\frac{\lambda}{\Gamma_x} + \frac{\lambda}{\Gamma_y}\right) \tag{5}$$

$$\begin{cases} \sin\dfrac{\varphi_1+\varphi_2}{2} = 1 \\ \sin\dfrac{\varphi_1-\varphi_2}{2} = 1 \end{cases} \tag{6}$$

where Γ_x is a period of the encoded metasurface in the x-direction, and Γ_y is a period of the encoded metasurface in the y-direction. The azimuthal angles and pitch angle for the quad beam are calculated from Equations (4) and (5) as $\psi = 45°$, $135°$, $225°$, $315°$, and $\theta = \sin^{-1}(\lambda)$.

In addition, according to the beam modulation function, when the unit coding sequence is received by the metasurface far-field scattering theory, the incident wave can be controlled to produce as many waves as possible after reflection. Therefore, the energy of a single directional beam will be significantly reduced, and the RCS will be effectively lowered. As a consequence, the designed frequency multiplexing unit has different functions to achieve beam splitting and RCS reduction in different frequency bands by sequence control.

For the design of the array structure, the perimeter of 250 mm was chosen to be ten times the wavelength corresponding to the lowest frequency point. The reason is that the array needs to maintain the scattering characteristics in the optical region. Moreover, the cross-shaped structure at the corners is formed by stitching together adjacent units. To satisfy the symmetry of the array structure and the integrity of the coding sequence, we designed the number of cross-shaped structures to be 25×25 and the number of V-shaped structures to be 24×24. The two frequency multiplexed encoded metasurfaces shown in Fig. 3 can be easily derived from the designed unit structure, the metasurface far-field scattering theory, and the design method for the encoded metasurface sequence described above. Fig. 3(a) shows a dual-frequency and dual beam splitting metasurface with the ability to double-split in two frequency bands. The low-band coding sequence at 12 GHz is arranged in the x-direction as "000111…" and the number of coding periods $\Gamma_x = 4$. In the high-frequency band at 20 GHz, the same coding sequence is implemented in the x-direction "000111…", the number of cycles $\Gamma_x = 4$. It can be seen that the azimuth angles of the reflected beam produced at 12 GHz and 20 GHz are $0°$ and $180°$. However, the pitch angle is determined by the frequency. When the frequency is equal to 12 GHz, the pitch angle of the reflected beam is $\pm 38.6°$; when the frequency is equal to 20 GHz, the pitch angle of the reflected beam is $\pm 22.2°$. Fig. 3(b) shows a dual-band RCS reduction and dual beam splitting metasurface, where the different beam control functions in the two bands are dominated by the coding sequence. In a disordered coding sequence at 12 GHz, the metasurface scatters the energy of the reflected wave in all directions in space, enabling the RCS reduction. At 20 GHz, the "010101…" code is assigned to the x-direction to achieve double beam splitting of the reflected waves on the metasurface, with beam azimuth angles of $0°$ and $180°$ and pitch angles of $\pm 47°$.

To demonstrate the far-field scattering properties of the coded metasurface, we construct the metasurface according to the coded sequence given in Fig. 3. The model is built in the full-wave

(a) (b)

Figure 3. The unit sequences of frequency multiplexed coded metasurface. (a) The sequences of dual-band and dual-beam split-beam metasurface; (b) The sequences of dual-frequency and dual-beam split-beam metasurface.

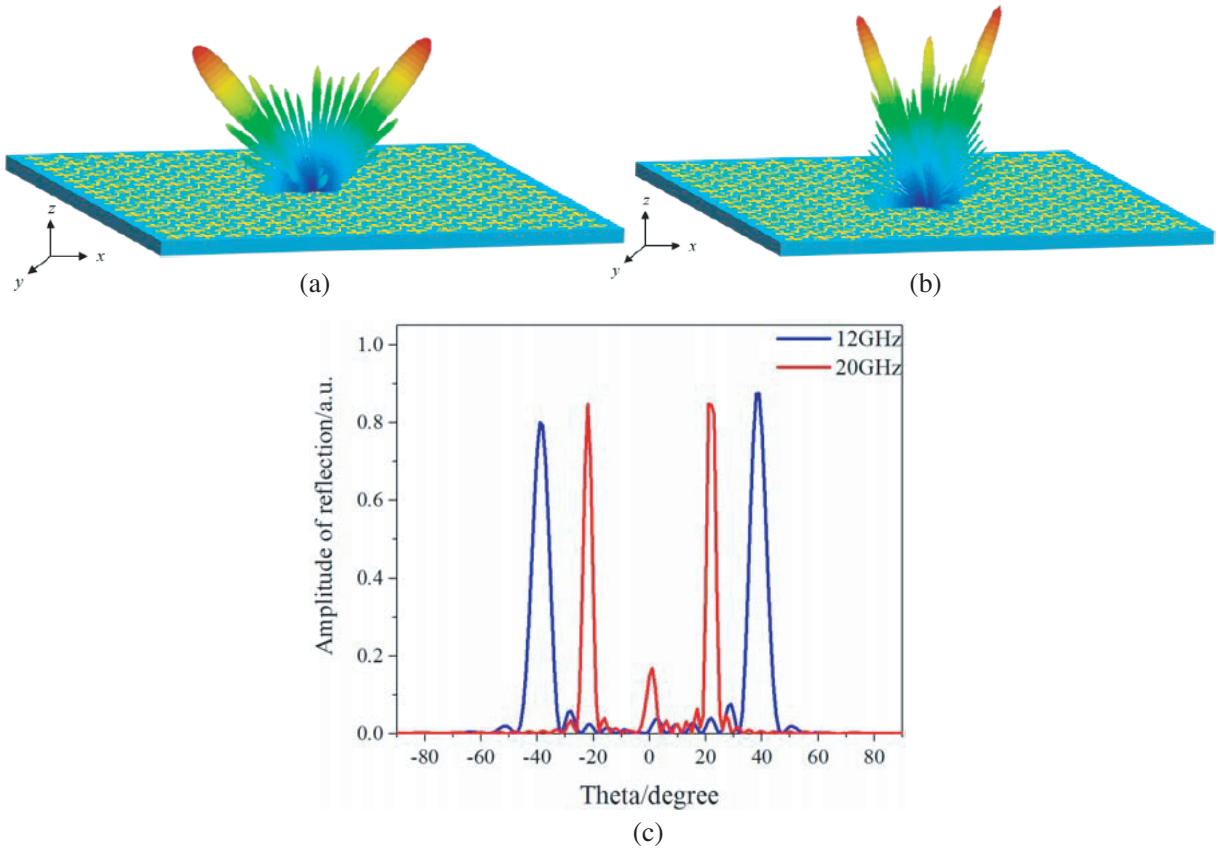

Figure 4. The far-field scattering map of encoded metasurface. (a) and (b) Three-dimensional far-field scattering map at 12 GHz and 20 GHz; (c) Two-dimensional far-field scattering map at 12 GHz and 20 GHz.

simulation software CST, and open boundary conditions are set in the x, y, and z directions to verify the far-field modes.

First, we investigate the dual-band beam splitting function of the frequency multiplexed metasurface sequence in Fig. 3(a). As shown in Fig. 4(a), far-field scatters from a y-polarised electromagnetic wave incident vertically at 12 GHz, which shows two symmetrical reflected beams of $\theta = 38.7°$, $\psi = 0°$ and $\theta = -38.7°$, $\psi = 0°$ after reflection from the metasurface. The comparative analysis with the theoretical values calculated by Equations (2), (3), (4) shows that the error of the simulation results is within 0.5°. Fig. 4(b) shows the far-field scattering at 20 GHz. Although the coding sequence is the same as in the low-frequency band, double symmetrical reflected waves with different angles of $\theta = 22.2°$, $\psi = 0°$ and $\theta = -22.1°$, $\psi = 180°$ are generated. Compared with the theoretical calculation value, the error is within 0.4°. The normalized two-dimensional scattering coefficients of the metasurface at 12 GHz and 20 GHz are both at 0.8 and above, as illustrated in Fig. 4(c). The dual-frequency multiplexed beam control function can be effectively implemented by the proposed metasurface in this paper.

We next investigate the metasurface sequence in Fig. 3(b) to achieve different functions in the

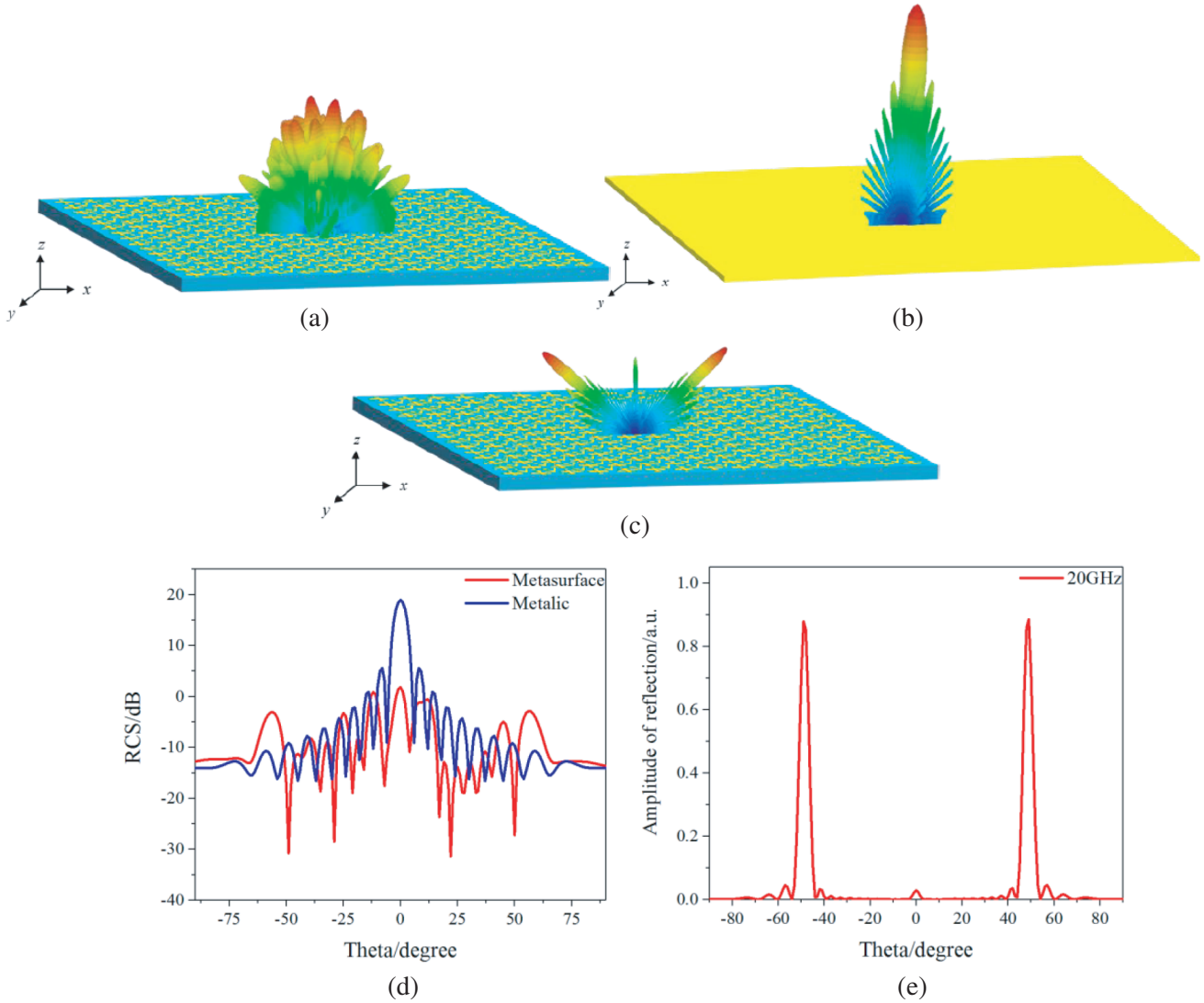

Figure 5. The far-field scattering map of the encoded metasurface. (a) The graph of encoded metasurface RCS reduction; (b) Total reflection graph of the metal plate; (c) 3-D far-field and 2-D scattering graph at 20 GHz; (d) Compared of RCS reduction effect at 12 GHz.

dual-band. The 3-D far-field scattering maps of encoded metasurfaces and the same-sized metal plates at 12 GHz are shown in Figs. 5(a) and (b). The reflected wave energy is effectively spread over the entire upper half of the space, and the beam energy in a single direction is considerably reduced. The reason is that when the units are arranged in an optimized sequence, their random phase distribution causes the reflection of the y-polarized incident wave to produce multiple beams. The maximum 11 dB reduction in metasurface RCS values compared to a metal plate of the same size is introduced in Fig. 5(d).

Additionally, Fig. 5(c) shows that the metasurface at 20 GHz disrupts the phase of the reflected wave in the normal direction, producing a double beam splitting. The metasurface normalized reflection diagram is presented in Fig. 5(e). The two main beams with angles $\theta = 47.6°$, $\psi = 0°$ and $\theta = -47.6°$, $\psi = 180°$, which approximate the theoretical values solved by Equations (2) and (3), are generated in the x-z plane. Meanwhile, the reflected electromagnetic beam in the normal direction is in low energy. Therefore, at 20 GHz, wave incidence and reflection at a predetermined angle can be implemented. Compared with [13–15], the frequency multiplexed metasurface designed in this paper can significantly reduce the mutual interference of parameters between operating bands, and the frequency band spacing is more prominent. In addition, the reflection amplitude of the unit structures is near 1, and the reflection of electromagnetic waves can be handled more flexibly.

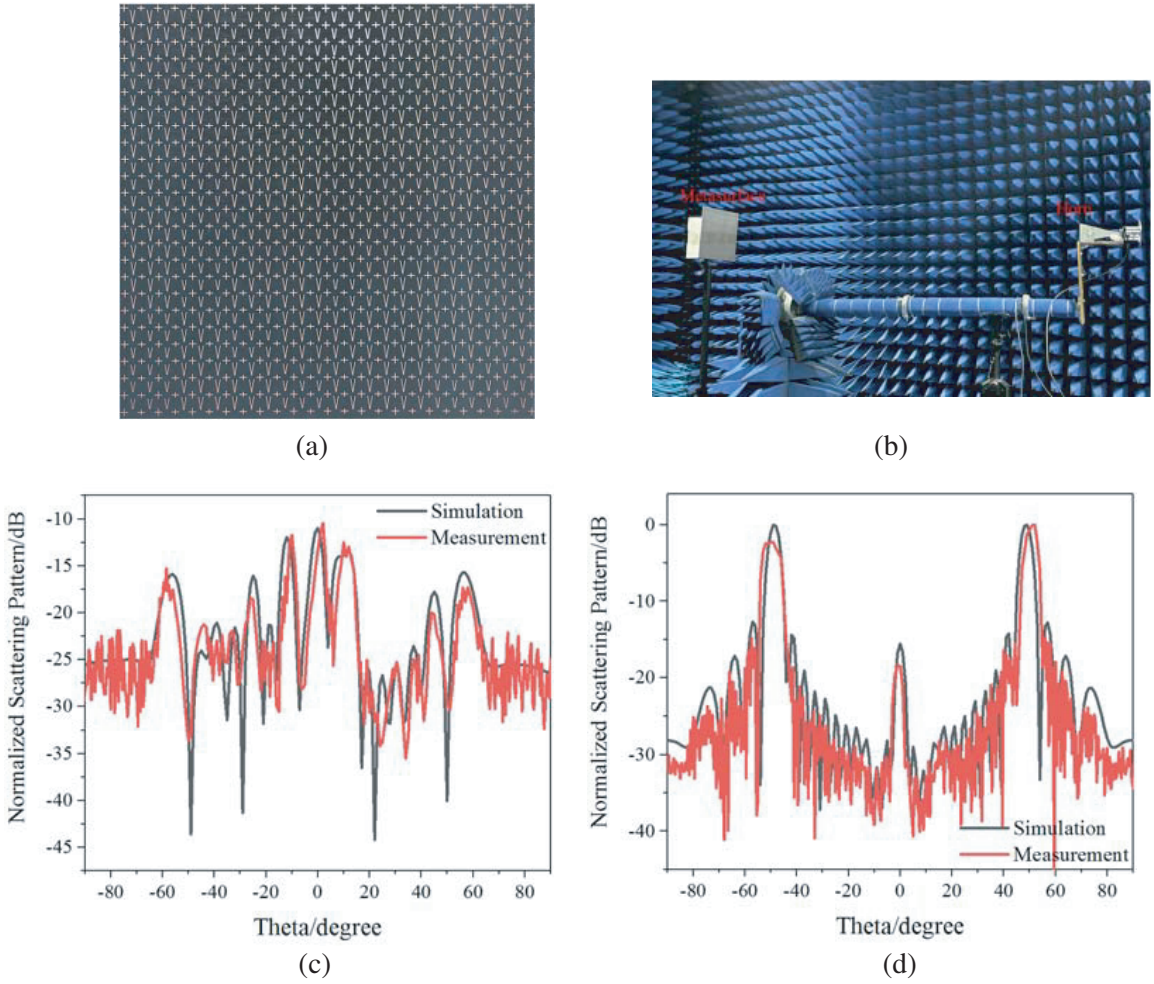

Figure 6. Fabricate and test. (a) Photo of the fabricated sample; (b) Experiment device; (c) and (d) Compared 12 GHz and 20 GHz far-field test and simulation results.

3. TEST AND DISCUSSION

Aiming to experimentally verify the frequency multiplexing coded metasurface design method and unit performance in this paper, a metasurface with RCS reduction in the low-frequency band and dual beam splitting in the high-frequency band is fabricated and measured.

As illustrated in Fig. 6(a), the sample is composed of 25×25 basic unit structures and has a size of $250\,\text{mm} \times 250\,\text{mm}$. The sample is tested in the far field in a standard microwave darkroom with the test system shown in Fig. 6(b). The sample, feed antenna, and receiving probe should have the same height. The feed antenna is 1.8 m in front of the metasurface, and the receiving probe is within the far-field distance of the metasurface. A comparison of the far-field scattering test and simulation results for frequency multiplexed coded metasurfaces at operating frequencies of 12 GHz and 20 GHz is shown in Figs. 6(c) and (d). The black curve in the diagram shows the simulated results, and the measured results are shown in red. The measured results demonstrate that at an incident wave frequency of 12 GHz, the metasurface achieves a relatively excellent RCS value reduction, with a slight difference of 0.6 dB from the simulation results. At an incident wave frequency of 20 GHz, the reflected wave at the metasurface has double beams with deflection angles of $\theta = 49.7°$, $\psi = 0°$ and $\theta = -49.7°$, $\psi = 0°$, which differs from the simulation results by about 2.1°. The measured results show excellent agreement with the simulated ones. Within the fault tolerance range, the designed coded metasurface can effectively realize multiplexing frequencies in the same aperture plane and achieve different beam control functions in the dual bands.

4. CONCLUSION

In summary, a unit design for a square F4B dielectric substrate with a copper-clad bottom surface and a V-shaped and four-cornered half-cross metal structure has been presented. Four 1-bit coding units operating in dual-frequency bands are optimized. In accordance with the functional setup and based on the theory of far-field scattering from metasurface, we design a frequency multiplexed coded metasurface to achieve RCS reduction in the low-frequency band and dual beams splitting in the high-frequency band. The metasurface is machined and tested. The experimental results are consistent with the simulation in CST. Notably, the design has the advantage of simple structure and flexible working frequency point and function setting, which effectively improves the problem of a single working frequency band and function of reflective type metasurface. On this basis, the metasurface design can be applied to other frequency bands as appropriate, combining methods such as sequence changes and new unit structures as well as polarisation states of the incident wave. It can realize frequency multiplexing functions such as multi-type aggregation, polarization conversion, and vortex electromagnetic wave generation. The design of frequency multiplexing metasurfaces has potential application value in future communication and other fields.

ACKNOWLEDGMENT

This work was supported by the Science and Technology Research Program of Chongqing Municipal Education Commission (Grant No. KJQN201800639).

REFERENCES

1. Saifullah, Y., et al., "Multi-bit dielectric coding metasurface for EM wave manipulation and anomalous reflection," *Optics Express*, Vol. 28, 1139–1149, 2019.
2. Wu, R. Y., L. Bao, and L. W. Wu, "Broadband transmission-type 1-bit coding metasurface for electromagnetic beam forming and scanning," *Mechanics and Astronomy*, Vol. 63, 284211, 2021.
3. Arbabi, E., A. Arbabi, and S. M. Kamali, "Multiwavelength polarization-insensitive lenses based on dielectric metasurfaces with meta-molecules," *Optica*, Vol. 3, 628–633, 2016.
4. Shen, Z., B. Jin, and J. Zhao, "Design of transmission-type coding metasurface and its application of beam forming," *Applied Physics Letters*, Vol. 109, 1119–1121, 2016.

5. Shang, G. Y. and H. Y. Li, "Coding metasurface holography with polarization-multiplexed functionality," *Journal of Applied Physics*, Vol. 129, 34–35, 2021.
6. Zhang, L. and X. Wan, "Realization of low scattering for a high-gain Fabry-Perot antenna using coding metasurface," *IEEE Transactions on Antennas and Propagation*, Vol. 65, 3374–3383, 2017.
7. Bai, G. D., Q. Ma, and I. Shahid, "Multitasking shared aperture enabled with multiband digital coding metasurface," *Advanced Optical Materials*, Vol. 6, 1–10, 2018.
8. Cui, T. J., M. Qi, and X. Wan, "Coding metamaterials, digital metamaterials and programming metamaterials," *Light: Science & Applications*, Vol. 3, 218, 2014.
9. Liu, S., T. J. Cui, and L. Zhang, "Convolution operations on coding metasurface to reach flexible and continuous controls of terahertz beams," *Advanced Science*, Vol. 3, 1600156, 2016.
10. Iqbal, S., H. Rajabalipanah, and L. Zhang, "Frequency-multiplexed pure-phase microwave meta-holograms using bi-spectral 2-bit coding metasurfaces," *Nanophotonics*, Vol. 9, 703–714, 2020.
11. Fu, C. and C. Liu, "Reflection-type 1-bit coding metasurface for RCS reduction combined diffusion and reflection," *Journal of Physics D Applied Physics*, Vol. 53, 5107, 2020.
12. Li, J., J. Feng, and B. Li, "Dual-band transmissive cross-polarization converter with extremely high polarization conversion ratio using transmitarray," *Materials*, Vol. 12, 1827, 2019.
13. Zhu, L., T. C. Li, and J. H. Huang, "Frequency coding all-dielectric metasurface for flexible control of electromagnetic radiation," *Applied Physics A*, Vol. 127, 131, 2021.
14. Xie, R., G. Zhai, and J. Gao, "Multifunctional geometric metasurfaces based on tri-spectral meta-atoms with completely independent phase modulations at three wavelengths," *Advanced Theory and Simulations*, Vol. 3, 2000090, 2020.
15. Lin, J., C. Chen, and J. Ding, "Dual-frequency multiple compact vortex beams generation based on single-layer Bi-spectral metasurface," *Applied Physics Letters*, Vol. 119, 081905, 2021.